

One-loop QCD corrections to the $e^+e^- \rightarrow W^+W^-b\bar{b}$ process at the ILC

Guo Lei, Ma Wen-Gan, Zhang Ren-You, and Wang Shao-Ming
Department of Modern Physics, University of Science and Technology
of China (USTC), Hefei, Anhui 230027, P.R.China

Abstract

We study the full contributions at the leading order(LO) and QCD next-to-leading order(NLO) to the cross section of the $e^+e^- \rightarrow W^+W^-b\bar{b}$ process in the standard model(SM) at the ILC. In dealing the resonance problem we adopted the complex mass scheme in both tree-level and one-loop level perturbative calculations. Our numerical results show that the K-factor varies from 1.501 to 0.847 when \sqrt{s} goes up from 360 *GeV* to 1.5 *TeV*. We investigate the dependence of the LO and QCD NLO corrected cross sections of process $e^+e^- \rightarrow W^+W^-b\bar{b}$ on colliding energy \sqrt{s} and Higgs-boson mass. We also present the results of the LO and QCD NLO corrected distributions of the transverse momenta of final particles, and the invariant masses of Wb -, $b\bar{b}$ - and WW -pair.

PACS: 13.66.Jn, 14.65.Ha, 14.80.Bn, 12.38.Bx

I. Introduction

The Higgs boson, which gives masses to the weak vector bosons and fermions, plays an important role in the standard model(SM). Unfortunately, it has not been directly detected yet in experiments. Searching for Higgs boson within the standard model(SM) and study the phenomenology concerning Higgs properties are the important tasks at the present and upcoming high energy colliders. LEP II experiments have provided the lower limit on the SM Higgs mass as 114.4 GeV at the 95% confidence level, which is extracted from the results of searches for $e^+e^- \rightarrow Z^0H^0$ production[1, 2]. While the indirect evidences of the SM Higgs mass through electroweak precision measurements indicate the 95% C.L. upper bound as $m_H \lesssim 182 \text{ GeV}$, when the lower limit on m_H is used in determination of this upper limit[2]. On the other hand, the heavy top-quark practically plays a central and crucial role in probing the electroweak symmetry breaking as well as the flavor problem in all the extended models beyond the SM which address the hierarchy problem. Recently, a new datum of top-quark mass has been already presented by the CDF and D0 experiments at Fermilab, and the preliminary world average mass of the top-quark is known as $m_t = 172.5 \pm 1.3(stat) \pm 1.9(syst) \text{ GeV}$, which corresponds to a 20% precision improvement relative to the previous combination[3].

The future International Linear Collider (ILC) is proposed by the particle physics community with the entire colliding energy in the range of $200 \text{ GeV} < \sqrt{s} < 500 \text{ GeV}$ and an integrated luminosity of around $500 (fb)^{-1}$ in four years. The machine should be upgradeable to $\sqrt{s} \sim 1 \text{ TeV}$ with an integrated luminosity of $1 (ab)^{-1}$ in three years[4]. Most of the main physics topics within the SM or its beyond at TeV energy scale can be explored at such a machine. Emphasis is given to the study of top-quark physics, electroweak physics in the SM, and the measurements in the extended SM, such as supersymmetry.

Compared with the hadron colliders, such as the Tevatron and the CERN Large Hadron Collider (LHC), the ILC can produce top and Higgs boson signal events more easily resolved from backgrounds. Therefore, the ILC is an ideal facility to study top and Higgs physics with much more precise measurement for their parameters. At the ILC we can also carry out the study of gauge boson interactions, and the delicate cancellations which are related to the gauge structure of the theory and essential to preserve unitarity. Furthermore, the ILC experiment might be able to

explore the signature of the new physics, if the SM is really only an effective theory at low energy.

At the ILC, detecting the top-quark pair production process $e^+e^- \rightarrow t\bar{t}$ is a good way to study the top-quark properties, and the associated Higgs production with Z^0 boson $e^+e^- \rightarrow H^0Z^0$ is one of the cleanest signature in discovering Higgs boson if the the b-quark trigger system has high performances except vertex detectors[5]. The former process will be followed by the subsequential decay through $t\bar{t} \rightarrow W^+W^-b\bar{b}$ [6], while the later process goes via $H^0Z^0 \rightarrow W^+W^-b\bar{b}$ through decays $H^0 \rightarrow W^+W^-$ and $Z^0 \rightarrow b\bar{b}$ if the Higgs boson mass is larger than $2m_W$ [7]. Therefore, the signature of $e^+e^- \rightarrow W^+W^-b\bar{b}$ at the ILC serves as non-resonant background to both top-quark pair production and associated production of Higgs boson with Z^0 boson. We can see that it is crucial to separate the top and Higgs signatures from the other $W^+W^-b\bar{b}$ production backgrounds in ILC experimental data analyzing. In the precise measurements of the signals of both the $t\bar{t}$ pair and H^0Z^0 associated production processes, the relevant irreducible background from $e^+e^- \rightarrow W^+W^-b\bar{b}$ should be carefully investigated.

In Refs.[6, 8, 9, 10, 11, 12] the NLO electroweak and QCD corrections to the process $e^+e^- \rightarrow t\bar{t}$ and decay $t \rightarrow W^+b$ have been already extensively studied. And the non-relativistic effect near the threshold of $t\bar{t}$ production is also studied carefully in Ref.[13], which can not be reliably described with fixed QCD orders in perturbative theory. The Higgs-strahlung Bjorken process $e^+e^- \rightarrow H^0Z^0$ was investigated in Ref.[14], and the process $e^+e^- \rightarrow t\bar{t} \rightarrow W^+W^-b\bar{b} \rightarrow 6f$ with six fermion final states after W pair decays has been also calculated at the lowest order in Ref.[15]. The evaluation of the $e^+e^- \rightarrow W^+W^-b\bar{b}$ process with finite width method at the tree-level is also presented in Ref. [7, 16]. All those studies indicate that the precise investigations of the characteristics of top-quark and the Higgs-boson are significant for the future e^+e^- ILC experiments.

In this paper we present the calculations of the cross section of the process $e^+e^- \rightarrow W^+W^-b\bar{b}$ at the leading order(LO) and its QCD next-to-leading order(NLO) ($\mathcal{O}(\alpha_s)$) corrections. The paper is organized as follows: In the following section we present the analytical calculations for process $e^+e^- \rightarrow W^+W^-b\bar{b}$ at the LO and QCD NLO. The verifications of the correctness of our calculations are declared in section III. The numerical results and discussions are given in section IV. In the last section we give a short summary.

II. Calculations

The calculations for the process $e^+e^- \rightarrow W^+W^-b\bar{b}$ are carried out in 't Hooft-Feynman gauge. In the QCD NLO calculations, we use the dimensional regularization(DR) method to isolate the ultraviolet(UV) and infrared(IR) singularities. In order to preserve gauge invariance, we adopt the approach of the complex mass scheme to deal with the unstable particles in the calculations for the tree-level cross section and QCD NLO radiative correction[17, 18]. The on-mass-shell(OS) scheme is used to renormalize the masses and fields of related bosons and fermions. The FeynArts3.2 package[19] is adopted to generate Feynman diagrams and convert them to corresponding amplitudes. The amplitude calculations are mainly implemented by applying FormCalc4.1 programs[20]. The formula for calculating the IR divergent integrals with complex internal masses in DR scheme are obtained by analytically extending the expressions in Ref.[21] to the complex plane. The numerical evaluations of IR safe one-point, two-point, three-point and four-point integrals with internal complex masses, are implemented by using the expressions analytically continued to complex plane from those presented in Refs.[22, 23]. And the 5-point scalar integral can be expressed in terms of multiple scalar four-point integrals[24]. The subroutines for one-loop integrals with complex masses are coded based on the LoopTools2.1[20] package which comes from FF library[25]. The $2 \rightarrow 4$ phase-space integration routine[27] is created based on the 2to3.F program in FormCalc4.1 package. The five-body phase-space integration for hard gluon radiation process $e^+e^- \rightarrow W^+W^-b\bar{b}g$ is accomplished by using CompHEP-4.4p3 program[26].

Now we present the analytically calculations of the tree-level cross section for $e^+e^- \rightarrow W^+W^-b\bar{b}$ and its QCD NLO radiative corrections. The notations for the process are defined as

$$e^+(p_1) + e^-(p_2) \rightarrow W^+(p_3) + W^-(p_4) + b(p_5) + \bar{b}(p_6), \quad (2.1)$$

where p_i ($i = 1 - 6$) label the four-momenta of incoming e^+ , e^- and outgoing final particles, respectively. There are 64 generic tree-level diagrams for the process $e^+e^- \rightarrow W^+W^-b\bar{b}$ presented in Fig.1, where internal wavy-line represents γ , Z^0 , or W^\pm and internal dash-line represents a Higgs-boson H^0 or a Goldstone $G^0(G^\pm)$. We can easily find that in Fig.1 there includes the tree-level diagrams for the processes $e^+e^- \rightarrow t^*\bar{t}^* \rightarrow W^+W^-b\bar{b}$ and $e^+e^- \rightarrow H^{0*}Z^{0*} \rightarrow W^+W^-b\bar{b}$.

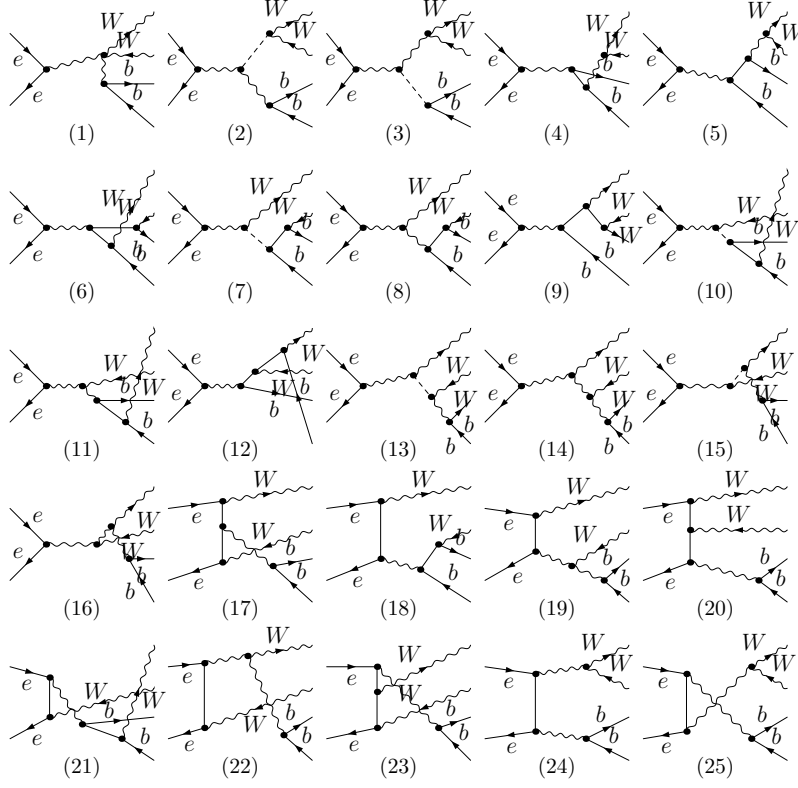


Figure 1: The generic tree-level Feynman diagrams for the $e^+e^- \rightarrow W^+W^-b\bar{b}$ process. Internal wavy-line represents γ -, Z^0 -, or W^\pm -propagator. Internal dash-line represents a Higgs boson H^0 or a Goldstone $G^0(G^\pm)$.

The differential cross section for the process $e^+e^- \rightarrow W^+W^-b\bar{b}$ at the tree-level is obtained by the tree-level is obtained by

$$d\sigma_{tree} = \frac{(2\pi)^4}{4\sqrt{(p_1 \cdot p_2)^2 - m_e^4}} \overline{\sum} |\mathcal{M}_{tree}|^2 d\Phi_4, \quad (2.2)$$

where $d\Phi_4$ is the four-body phase space element given by

$$d\Phi_4 = \delta^{(4)}\left(p_1 + p_2 - \sum_{i=3}^6 p_i\right) \prod_{i=3}^6 \frac{d^3p_i}{(2\pi)^3 2E_i}. \quad (2.3)$$

The summation in Eq.(2.2) is taken over the spins and colors of final states, and the bar over the summation recalls averaging over initial spin states. In the calculation, the internal Z^0 and Higgs boson can be real, and the top-quark propagator can also be resonance when $\sqrt{s} > 2m_t$. To deal with these resonant singularities, we use the so-called complex mass scheme(CMS) in our perturbative calculations[17, 18]. The complex masses of W-, Z-, H-boson and top-quark are defined

as

$$\mu_X^2 = m_X^2 - im_X\Gamma_X, \quad (X = W, Z, H, t). \quad (2.4)$$

In the CMS approach the complex masses for all related unstable particles should be taken everywhere in both tree-level and one-loop level calculations. Then the gauge invariance can be conserved and singularity poles of propagators are avoided.

In calculating the complete QCD NLO corrections, we should consider the contributions of 30 self-energy diagrams, 94 triangle diagrams, 17 box diagrams and 6 pentagon diagrams. As a representative selection, we present the pentagon Feynman diagrams of the $e^+e^- \rightarrow W^+W^-b\bar{b}$ process in Fig.2. We adopt the Eqs.(4.26) and (4.27) in Ref.[18] for the renormalized QCD self-energy and counter-terms of top-quark with complex mass neglecting terms of $O(\alpha_s^2)$ by using OS-scheme.

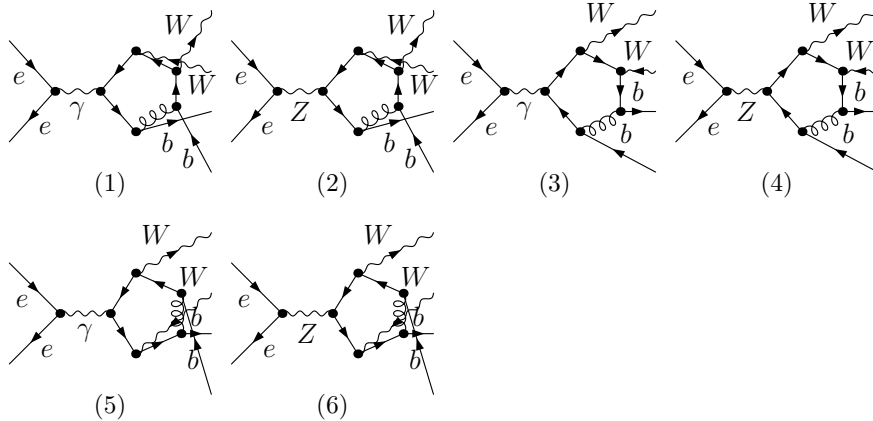


Figure 2: The pentagon Feynman diagrams for the $e^+e^- \rightarrow W^+W^-b\bar{b}$ process.

There exist both ultraviolet(UV) divergency and infrared(IR) soft singularity in the contributions of the QCD one-loop diagrams for $e^+e^- \rightarrow W^+W^-b\bar{b}$ process, but no collinear IR singularity due to the massive top- and bottom-quark. After doing the renormalization procedure, the UV singularity is vanished.

To cancel the IR soft divergency appeared in the virtual correction, we should consider the contribution of the real gluon emission process $e^+e^- \rightarrow W^+W^-b\bar{b}g$. We denote the real gluon emission process as

$$e^+(p_1) + e^-(p_2) \rightarrow W^+(p_3) + W^-(p_4) + b(p_5) + \bar{b}(p_6) + g(p_7). \quad (2.5)$$

To calculate the contribution of this process, we introduce an arbitrary small soft cutoff δ_s to separate its 5-body phase-space into two regions[28], i.e., soft($E_7 \leq \delta_s \sqrt{s}/2$) and hard($E_7 > \delta_s \sqrt{s}/2$) regions. After adopting the soft gluon approximation, the expression of σ_{soft} for $e^+e^- \rightarrow W^+W^-b\bar{b}g$ process with soft gluon has the form as

$$d\sigma_{soft} = C_F \frac{\alpha_s}{2\pi} g_{56} d\sigma_{tree}, \quad (2.6)$$

where $C_F = 4/3$ and g_{56} are defined as:

$$g_{56} = \left(\frac{\pi\mu^2}{\Delta E^2} \right)^\epsilon \Gamma(1+\epsilon) \left[\frac{4(p_5 \cdot p_6)}{\lambda^{1/2}(s_{56}, m_b^2, m_b^2)} \ln(\sigma) + 2 \right] \frac{1}{\epsilon} - \frac{2(p_5 \cdot p_6)}{\lambda^{1/2}(s_{56}, m_b^2, m_b^2)} \\ \times [\ln^2(\sigma) + 4Li_2(1-\sigma)] - \frac{2}{\rho} \ln \sigma + \mathcal{O}(\epsilon). \quad (2.7)$$

In above equation, $\lambda(s_{56}, m_b^2, m_b^2)$ is the kinematical function defined by:

$$\lambda(x, y, z) = x^2 + y^2 + z^2 - 2xy - 2yz - 2zx, \quad (2.8)$$

$\Delta E = E_7 = \delta_s \sqrt{s}/2$, $s_{56} = (p_5 + p_6)^2$ and

$$\rho = \frac{\lambda^{1/2}(s_{56}, m_b^2, m_b^2)}{s_{56}}, \quad \sigma = \frac{1-\rho}{1+\rho}. \quad (2.9)$$

Our created $2 \rightarrow 4$ phase space integration routine[27], is adopted in the tree-level and one-loop level calculations for $e^+e^- \rightarrow W^+W^-b\bar{b}$ process. The IR singularity part of the soft gluon emission process $e^+e^- \rightarrow W^+W^-b\bar{b}(g)$ can be exactly cancelled by the IR singularity induced by the one-loop virtual gluon correction. We apply CompHEP-4.4p3 program[26] to implement the phase space integration of the hard gluon emission process $e^+e^- \rightarrow W^+W^-b\bar{b} + g$. Finally, we get the finite total cross section including complete NLO QCD corrections for the process $e^+e^- \rightarrow W^+W^-b\bar{b}$ by summing up all the contribution parts,

$$\sigma_{NLO} = \sigma_{tree} + \sigma_{virtual} + \sigma_{soft} + \sigma_{hard}. \quad (2.10)$$

III. Checks

We have performed the following checks to prove the reliability of our calculation:

$m_t(GeV)$	$\sigma_{LO}(fb)(Ref.[16])$	$\sigma_{LO}(fb)(Comphep)$	$\sigma_{LO}(fb)$ (ours)
150	663.11	663.03(1±0.05%)	663.19(1±0.05%)
180	576.26	576.19(1±0.04%)	576.52(1±0.04%)
200	497.63	497.58(1±0.04%)	497.68(1±0.04%)

Table 1: The comparison of the numerical results of LO cross section neglecting the diagrams with Higgs-boson interchanging by using CompHEP-4.4p3 system, our in-house $2 \rightarrow 4$ phase-space integration routine with the corresponding selected results presented in Ref.[16] when $\sqrt{s} = 500 GeV$.

- The LO cross section for the process $e^+e^- \rightarrow W^+W^-b\bar{b}$ is calculated in the conditions of taking $\sqrt{s} = 500 GeV$ and neglecting the contribution of the diagrams with internal Higgs-boson exchange which are taken in Ref.[16]. The numerical results of the LO cross section for the process $e^+e^- \rightarrow W^+W^-b\bar{b}$ are listed in Table 1. There our results are obtained by using both CompHEP-4.4p3 program and our created $2 \rightarrow 4$ phase-space integration routine, and compared with the corresponding ones presented in Ref.[16]. We can see there is a good agreement between ours and those presented in Ref.[16]. The in-house $2 \rightarrow 4$ phase-space integration routine was also once verified in our previous work[27].
- We use our created codes for numerical evaluation of the one-loop integrals with complex internal masses. The comparisons are made between the results and those obtained by doing directly the integration of Feynman-parameter. There exists a good agreement. The results from both calculations for scalar two-, three-, four-point integrals are coincident with each other at least up to six digits, respectively.
- The exact cancellations of UV- and IR-divergencies are verified both analytically and numerically in our calculation.
- The independence of the total cross section including the NLO QCD corrections on the soft cutoff $\delta_s(= 2 \Delta E/\sqrt{s})$ is confirmed numerically. Our calculation shows the errors of the independence are less than 0.6% in the δ_s region of $[10^{-4}, 5 \times 10^{-2}]$. In further numerical calculation we fix $\delta_s = 10^{-3}$.
- In the following section, we shall clarify other verifications.

IV. Numerical results and discussion

In our numerical calculation we take the following input parameters[29, 30]:

$$\begin{aligned} \alpha(m_Z)^{-1} &= 127.918, & \alpha_s(m_Z^2) &= 0.1176, & m_Z &= 91.1876 \text{ GeV}, \\ m_W &= 80.403 \text{ GeV}, & \Gamma_Z &= 2.495 \text{ GeV}, & \Gamma_W &= 2.141 \text{ GeV}, \\ m_t &= 172.5 \text{ GeV}, & m_b &= 4.7 \text{ GeV}, & m_e &= 0.5109991 \text{ MeV}. \end{aligned} \quad (4.1)$$

Due to the application of the CMS approach, we use the complex weak mixing angle defined as

$$c_w^2 = 1 - s_w^2 = \frac{\mu_W^2}{\mu_Z^2}. \quad (4.2)$$

In our LO and NLO numerical calculations we set the QCD renormalization scale μ as $\mu = m_W + m_b$, and take the strong coupling $\alpha_s(\mu^2) = 0.11885$, which is obtained by using the formula at three-loop level (\overline{MS} scheme) with the five active flavors[29].

Since the widths of top-quark and Higgs boson haven't been well provided or measured experimentally by now, we use their theoretical results from perturbative calculations. Considering the fact that top-quark mass is above $m_W + m_b$, and $V_{tb} \sim 1$, the decay of top-quark is dominated by undergoing two-body decay $t \rightarrow W^+b$, and the total decay width of top-quark is approximately equal to the decay width of $t \rightarrow W^+b$. Neglecting terms of order m_b^2/m_t^2 , α_s^2 and $(\alpha_s/\pi)M_W^2/m_t^2$, the width predicted in the SM is [31]:

$$\Gamma_t = \frac{\alpha m_t^3}{16m_W^2(1 - m_W^2/m_Z^2)} \left(1 - \frac{m_W^2}{m_t^2}\right)^2 \left(1 + 2\frac{m_W^2}{m_t^2}\right) \left[1 - \frac{2\alpha_s}{3\pi} \left(\frac{2\pi^2}{3} - \frac{5}{2}\right)\right]. \quad (4.3)$$

The reasonable physical decay width of Higgs boson is obtained by employing the program Hdecay[32], where the partial decay width $\Gamma(H^0 \rightarrow q\bar{q})$ is calculated including $\mathcal{O}(\alpha_s^3)$ QCD radiative corrections. Then we obtain $\Gamma_t = 1.3745 \text{ GeV}$, $\Gamma_H(m_H = 120 \text{ GeV}) = 0.3692 \times 10^{-2} \text{ GeV}$ and $\Gamma_H(m_H = 180 \text{ GeV}) = 0.6286 \text{ GeV}$.

The numerical results of the LO, QCD NLO corrected cross sections and the corresponding K-factor($K \equiv \frac{\sigma_{NLO}}{\sigma_{LO}}$) for the process $e^+e^- \rightarrow W^+W^-b\bar{b}$ are plotted in Figs.3(a) and (b) respectively, when $m_H = 120 \text{ GeV}$. As indicated in Fig.3(a), both curves for the cross sections at the LO and NLO increase quickly in the \sqrt{s} region of $[350 \text{ GeV}, 400 \text{ GeV}]$ and decrease when $\sqrt{s} > 430 \text{ GeV}$. Fig.3(b) shows that the corresponding K-factor decreases slowly from 1.501 to 0.847 as \sqrt{s} running from 360 GeV to 1.5 TeV . The large positive peak near the $t\bar{t}$ threshold in Fig.3(b) is due to a

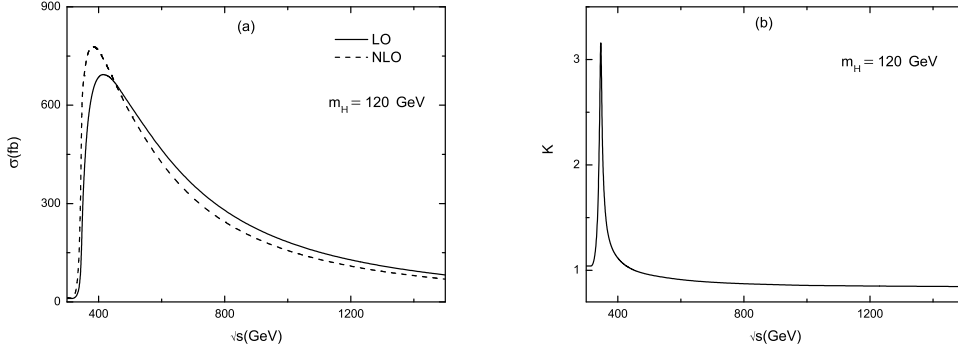


Figure 3: (a) The LO and NLO QCD corrected cross sections for the process $e^+e^- \rightarrow W^+W^-b\bar{b}$ as the functions of c.m.s. colliding energy(\sqrt{s}) with $m_H = 120 \text{ GeV}$, (b) the corresponding K-factor versus \sqrt{s} .

$\sqrt{s}(GeV)$	$\sigma_{tree}(fb)$	$\sigma_{NLO}(fb)$	K-factor
500	602.57(1±0.05%)	575.5(1± 0.38 %)	0.955(4)
1000	182.24(1±0.04%)	156.7(1± 0.38 %)	0.860(4)
1500	82.73(1±0.04%)	70.1(1± 0.37 %)	0.847(4)

Table 2: The LO and NLO QCD corrected cross sections, K-factors for $e^+e^- \rightarrow W^+W^-b\bar{b}$ process with $m_H = 120 \text{ GeV}$ and $\sqrt{s} = 500 \text{ GeV}$, 1000 GeV , 1500 GeV , respectively.

Coulomb singularity effect coming from the instantaneous gluon exchange between heavy quarks which has a small spatial momentum. In Table 2 we list the values of σ_{tree} , σ_{NLO} and K-factor at some typical \sqrt{s} points, which are read out from Figs.3(a-b). Since the QCD correction to the $e^+e^- \rightarrow W^+W^-b\bar{b}$ process with high colliding energy can be approximately decomposed into the QCD correction to the $t\bar{t}$ production plus the corrections to the $t(\bar{t}) \rightarrow W^+b(W^-b)$ decays when $m_H < 2m_W$, we make following verification to check our results. We evaluate the QCD correction to $e^+e^- \rightarrow W^+W^-b\bar{b}$ process by combining the QCD corrections to $e^+e^- \rightarrow t\bar{t}$ production and $t(\bar{t}) \rightarrow W^+b(W^-b)$ decays together, and get the K-factors to process $e^+e^- \rightarrow W^+W^-b\bar{b}$ as 0.8562(1) for $\sqrt{s} = 1 \text{ TeV}$ and 0.8433(1) for $\sqrt{s} = 1.5 \text{ TeV}$, which are coincident with the corresponding ones in Table 2 in error ranges.

In Fig.4(a) we present the plot of the LO and QCD NLO corrected cross sections as the functions of Higgs-boson mass, with $\sqrt{s} = 500 \text{ GeV}$ and m_H running form 60 GeV to 200 GeV . We find from Fig.4(a) that the LO and QCD NLO corrected cross sections are non-sensitive to the Higgs-boson

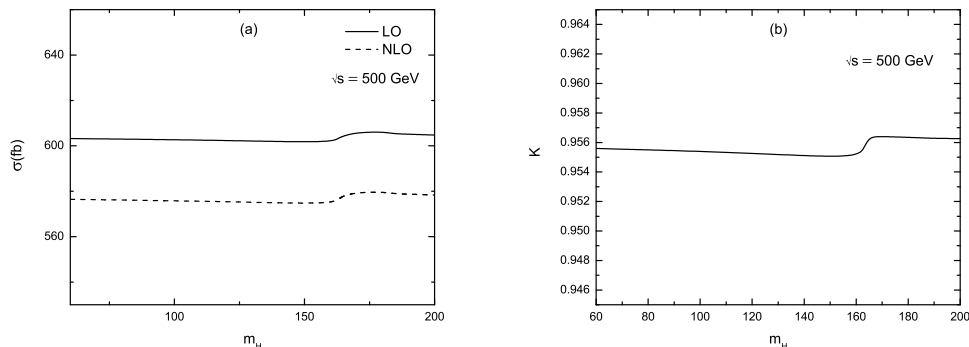


Figure 4: (a) The LO and QCD NLO corrected cross sections for the process $e^+e^- \rightarrow W^+W^-b\bar{b}$ as the functions of Higgs mass(m_H) with $\sqrt{s} = 500$ GeV. (b) The corresponding relative QCD NLO corrections versus m_H .

mass except in the vicinity of $m_H \sim 2m_W$, from there the Higgs mass becomes larger than $2m_W$, and H^0 -, Z^0 -boson are simultaneously resonances. We can see also from the figures that the contribution via $e^+e^- \rightarrow t^*\bar{t}^* \rightarrow W^+W^-b\bar{b}$ channel is much larger than that from $e^+e^- \rightarrow H^{0*}Z^{0*} \rightarrow W^+W^-b\bar{b}$ as concluded in Ref.[16]. Fig.4(b) shows the corresponding K-factor has the values around 0.956 in the range of $m_H \in [60$ GeV, 200 GeV].

Due to the CP-conservation, the distributions of transverse momenta of W^- -boson and \bar{b} quark should be the same as those of $p_T^{W^+}$ and p_T^b , respectively. We only present the distributions of the $p_T^{W^+}$ and p_T^b with $m_H = 120$ GeV and $\sqrt{s} = 500$ GeV in Figs.5(a) and (b). In these two figures we can see that the QCD NLO corrections suppress the LO differential cross sections $d\sigma_{LO}/dp_T^{W^+}$ and $d\sigma_{LO}/dp_T^b$. They also show that the differential cross sections of $d\sigma_{LO,NLO}/dp_T^{W^+}$ and $d\sigma_{LO,NLO}/dp_T^b$ have their maximal values at about $p_T^{W^+} \sim 70$ GeV and $p_T^b \sim 30$ GeV respectively. We see that the line shapes of the differential cross sections in these two figures are mainly determined by the contributions of the of $e^+e^- \rightarrow t^*\bar{t}^* \rightarrow W^+W^-b\bar{b}$ production.

We plot the invariant mass distributions of (W^+b) -pair, denoted as $M_{(W^+b)}$, at the LO and QCD NLO in Fig.6 with $m_H = 120$ GeV and $\sqrt{s} = 500$ GeV. The distribution of $M_{(W^-b)}$ should be the same as that of (W^+b) -pair due to the CP-conservation. We can see from the figure that most of the events are concentrated around a peak located at the position of $M_{(W^+b)} \sim m_t$. That demonstrates again the main contribution to the cross section of the process $e^+e^- \rightarrow W^+W^-b\bar{b}$

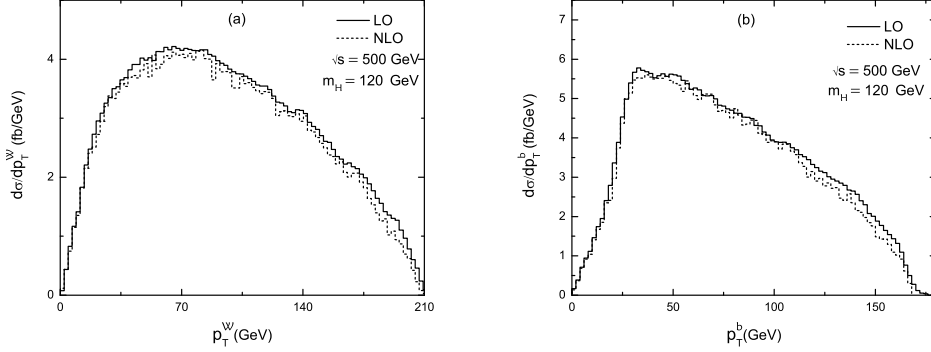


Figure 5: The distributions of the transverse momenta of W^+ and bottom-quark for the $e^+e^- \rightarrow W^+W^-b\bar{b}$ process at the LO and QCD NLO with $\sqrt{s} = 500 \text{ GeV}$ and $m_H = 120 \text{ GeV}$. (a) for W^+ , (b) for bottom-quark.

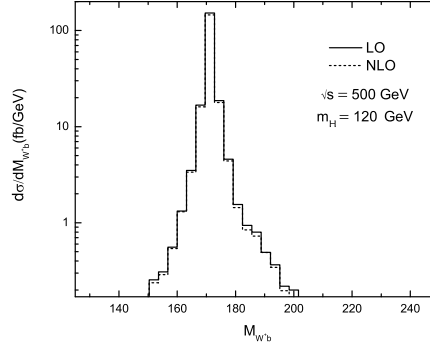


Figure 6: The distributions of the invariant mass of (W^+b) -pair (or $(W^-\bar{b})$ -pair) at the LO and QCD NLO with $m_H = 120 \text{ GeV}$ and $\sqrt{s} = 500 \text{ GeV}$.

with high colliding energy, is from top-pair production channel $e^+e^- \rightarrow t\bar{t}$ and followed by the decay of $t(\bar{t}) \rightarrow W^+b(W^-\bar{b})$. Here we can see that the QCD NLO correction slightly suppresses the LO differential cross section $d\sigma_{LO}/dM_{(W^+b)}$.

As we know, if Higgs boson has a mass larger than $2m_W$, the $e^+e^- \rightarrow H^{0*}Z^{0*} \rightarrow W^+W^-b\bar{b}$ channel will certainly slightly increase both the LO and QCD NLO corrected cross sections for $W^+W^-b\bar{b}$ production due to the Higgs-boson resonant effect as shown in Fig.4(a). It will bring a spike on the distribution of the (W^+W^-) -pair invariant mass at the position of $M_{(WW)} = m_H$. Analogously, the associated real Z^0 -boson produced via $e^+e^- \rightarrow H^0Z^0$ will induce a spike on the distribution of the invariant mass $M_{(b\bar{b})}$ at the position of $M_{(b\bar{b})} = m_Z$. In Figs.7(a) and (b) we

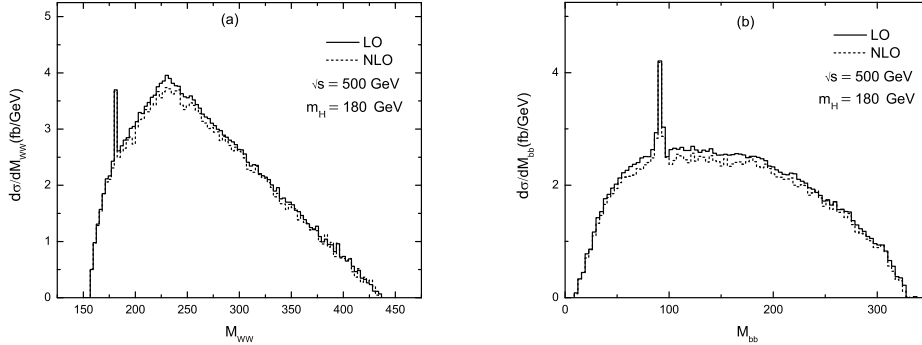


Figure 7: The distributions of the invariant masses of $(b\bar{b})$ -pair and (WW) -pair with $m_H = 180 \text{ GeV}$ and $\sqrt{s} = 500 \text{ GeV}$. (a) is for (WW) -pair, (b) is for $(b\bar{b})$ -pair.

show the the distributions of the WW - and $b\bar{b}$ -pair invariant masses with $\sqrt{s} = 500 \text{ GeV}$ and $m_H = 180 \text{ GeV}$, respectively. We can see spikes around the vicinities of $M_{(WW)} \sim m_H \sim 180 \text{ GeV}$ and $M_{(b\bar{b})} \sim m_Z \sim 90 \text{ GeV}$ in Fig.7(a) and Fig.7(b) respectively, which may be used to distinguish the $e^+e^- \rightarrow H^0 Z^0 \rightarrow W^+W^-b\bar{b}$ signature from the corresponding irreducible background $e^+e^- \rightarrow W^+W^-b\bar{b}$. It shows also the QCD NLO correction obviously modifies the LO differential cross sections of $d\sigma_{LO}/dM_{(WW)}$ and $d\sigma_{LO}/dM_{(b\bar{b})}$.

Theoretically, the NLO QCD correction to the process $e^+e^- \rightarrow Z^0 H^0 \rightarrow W^+W^-b\bar{b}$ with real Z^0 - and Higgs-boson as intermediate particles, should be determined only by the NLO QCD corrections to the $Z^0 \rightarrow b\bar{b}$ decay. As a check to verify our calculations, we also calculate the correction to the decay $Z^0 \rightarrow b\bar{b}$ with $\sqrt{s} = 500 \text{ GeV}$ and $m_H = 180 \text{ GeV} > 2m_W$ and get the K-factors for $e^+e^- \rightarrow Z^{0*} H^{0*} \rightarrow W^+W^-b\bar{b}$ process being 1.0466(1), which is coincident with the result by calculating the $e^+e^- \rightarrow Z^{0*} H^{0*} \rightarrow W^+W^-b\bar{b}$ process with full QCD NLO diagrams, where the K-factors are 1.046(2).

V. Summary

In this paper we calculate the complete one-loop QCD corrections in the SM to the process $e^+e^- \rightarrow W^+W^-b\bar{b}$ at the ILC. We study the dependence of the LO and QCD NLO corrected cross sections of process $e^+e^- \rightarrow W^+W^-b\bar{b}$ on colliding energy \sqrt{s} and Higgs-boson mass. We investigate the LO and QCD NLO corrected distributions of the transverse momenta of final particles and the

LO and QCD NLO corrected differential cross sections of invariant masses of Wb -, $b\bar{b}$ - and WW -pair. It shows that NLO QCD correction obviously modifies the LO cross section of the process $e^+e^- \rightarrow W^+W^-b\bar{b}$, and when the colliding energy \sqrt{s} goes up from 360 GeV to 1.5 TeV, the K-factor varies from 1.501 to 0.847. The numerical results show that if $m_H > 2m_W$, the resonant effect of H^0 -boson appearing in the $e^+e^- \rightarrow H^0Z^0 \rightarrow W^+W^-b\bar{b}$ channel will induce a little enhancement to the LO and QCD NLO corrected cross sections for $e^+e^- \rightarrow W^+W^-b\bar{b}$ process. We find that it may be possible to select the $e^+e^- \rightarrow H^0Z^0 \rightarrow W^+W^-b\bar{b}$ events from the corresponding irreducible background $e^+e^- \rightarrow W^+W^-b\bar{b}$ which is dominantly produced by the $e^+e^- \rightarrow t\bar{t} \rightarrow W^+W^-b\bar{b}$ channel by analyzing the invariant masses of final WW - and $b\bar{b}$ -pair.

Acknowledgments: This work was supported in part by the National Natural Science Foundation of China, Specialized Research Fund for the Doctoral Program of Higher Education(SRFDP) and a special fund sponsored by Chinese Academy of Sciences.

References

- [1] R.Barate et al., Phys. Lett. **B565** (2003) 61.
- [2] The LEP Collaborations ALEPH, DELPHI, L3, OPAL, and the LEP Electroweak Working Group. LEPEWWG/2007-01 and arXiv:0712.0929.
- [3] Tevatron Electroweak Working Group(for the CDF and D0 Collaborations), Fermilab-TM-2347-E, TEVEWWG/top 2006/01, CDF-8162, D0-5064, hep-ex/0603039v1.
- [4] Parameters for Linear Collider, http://www.fnal.gov/directorate/icfa/LC_parameters.pdf
- [5] Proceedings of the Workshop on "High Luminosities at LEP", CERN Report 91-02, Geneva, Switzerland.
- [6] I. Bigi, H. Krasemann, Z. Phys. **C7** (1981) 127; J. Kühn, Acta.-Phys.-Austr. (Suppl.) **XXIV** (1982) 203; I. Bigi, Y. Dokshitzer, V. Khoze, J. Kühn and P. Zerwas Phys. Lett. **B181** (1986) 157.
- [7] A. Ballestrero, E. Maina, S. Moretti, Phys. Lett. **B335** (1994)460.

- [8] R. Kleiss and W.J. Stirling, Z. Phys. **C40** (1988) 419;
- [9] J. Jersak, E. Laerman, P.M. Zerwas, Phys. Rev. **D25**(1980)1218; S. Güsken, J.H. Kühn, P.M. Zerwas, Phys. Lett. **B155**(1985)185; J.H. Kühn, P.M. Zerwas, Phys. Rep. **167**(1988)321; V.S. Fadin, V.A. Khoze, Pi'sma v Zh. Eksp. Teor. Fiz. **46**(1987)417; Yad. Fiz.**48**(1988)487; V.S. Fadin, V.A. Khoze, T. Sjöstrand, Z. Phys. **C48**(1990)613; V.S. Fadin, O.I. Yakovlev, Novosibirsk preprint IYF 90-138 (1990); W. Kwong, Phys. Rev. **D43**(1991)1488; H. Inazawa,, T. Morii, J. Morishita, Phys. Lett. **B203**(1988)279; Z. Phys. **C42**(1989)569; K. Hagiwara et al., Nucl. Phys. **B344**(1990)1; J. Feigenbaum, Phys. Rev. **D43**(1991)264; M.J. Strassler, M.E. Peskin, Phys. Rev. **D43**(1991)1500; J.H. Kühn, Proceedings of the *Workshop on on Physics and Experiments with Linear e^+e^- Colliders*, Waikoloa, Hawaii 1993, eds.: F.A. Harris, S.L. Olsen, S. Pakvasa, X. Tata.
- [10] W. Beenakker, W. Hollik and S.C. van der Marck, Nucl. Phys. **B365**(1991)24.
- [11] A.A. Akhundov, D.Y. Bardin and A. Leike, Phys. Lett. **B261**(1991)321; A. Arbuzov, D. Bardin, A. Leike, Mod. Phys. Lett. **A7** (1992) 2029; E: **A9** (1994) 1515.
- [12] A. Denner and T. Sack, Nucl. Phys. **B358** (1991) 46; W. Beenakker, S.C. van der Marck and W. Hollik, Nucl. Phys. **B365** (1991) 24; W. Beenakker and W. Hollik, Phys. Lett. **B269**(1991)425.
- [13] Adrian Signer, hep-ph/0604032; Andre H. Hoang, hep-ph/0604185; Y. Kiyo, hep-ph/0602064; D. Eiras, M. Steinhauser, Nucl.Phys. **B757** (2006) 197.
- [14] W.Kilian, M.Krammer, P.M. Zerwas, Phys. Lett. **B373**(1996)135, "Higgs Physics at Lep-2", in CERN LEP-2 yellow report vol.1, CERN-96-01, hep-ph/9602250; J. Fleischer and F. Jegerlehner, Nucl. Phys. **B216** (1983) 469; B. A. Kniehl, Z. Phys. **C55** (1992) 605; A. Denner, J. Kblbeck, R. Mertig, M. Boehm, Z. Phys. **C56** (1992) 261.
- [15] F. Yuasa, Y. Kurihara, S. Kawabata, Phys. Lett. **B414** (1997) 178; Elena Accomando, Alessandro Ballestrero, Marco Pizzio, Nucl. Phys. **B512** (1998) 19; F. Gangemi, G. Montagna, M. Moretti, O. Nicosini, F. Piccinini, Nucl.Phys. **B559** (1999) 3; Karol Kolodziej, Eur. Phys.J. **C23** (2002) 471; Stefan Dittmaier, Markus Roth, Nucl. Phys. **B642** (2002) 307.

- [16] A. Ballestrero, E. Maina, S. Moretti, Phys. Lett. **B333**(1994) 434.
- [17] A. Denner, S. Dittmaier, M. Roth, D. Wackerath, Nucl. Phys. **B560** (1999) 33.
- [18] A. Denner, S. Dittmaier, M. Roth, L.H. Wieders, Nucl. Phys. **B724** (2005) 247.
- [19] T. Hahn, Comput. Phys. Commun. **140** (2001)418.
- [20] T. Hahn, M. Perez-Victoria, Comput. Phys. Commun. **118** (1999)153.
- [21] W. Beenakker, H. Kuijf, W.L. van Neerven and J. Smith, Phys. Rev. **D40** (1989) 54; Stefan Dittmaier, Nucl.Phys. B675 (2003) 447.
- [22] G.'t Hooft and M. Veltman, Nucl. Phys. **B153** (1979) 365.
- [23] A. Denner, U Nierste and R Scharf, Nucl. Phys. **B367** (1991) 637.
- [24] A. Denner and S. Dittmaier, Nucl. Phys. **B658** (2003) 175.
- [25] G. J. van Oldenborgh, NIKHEF-H/90-15.
- [26] E. Boos, V. Bunichev, et al., (the CompHEP collaboration), Nucl. Instrum. Meth. **A534** (2004) 250-259, hep-ph/0403113.
- [27] Guo Lei, Ma Wen-Gan, Han Liang, Zhang Ren-You, Jiang Yi, Phys. Lett. **B654** (2007) 13.
- [28] B. W. Harris and J.F. Owens, Phys. Rev. **D65** (2002) 094032, hep-ph/0102128.
- [29] W.M. Yao, et al., J. of Phys. **G33**,1 (2006).
- [30] F. Jegerlehner, DESY 01-029, hep-ph/0105283.
- [31] M. Jezabek and J.H. Kühn, Nucl. Phys. **B314** (1989) 1.
- [32] A. Djouadi, J. Kalinowski, M. Spira, Comput. Phys. Commun. 108 (1998) 56.